Spin Density Encodes Intramolecular Singlet Exciton Fission in Pentacene Dimers

KC Krishnapriya,[1†] Palas Roy,[2†] Boregowda Puttaraju,[1] Ulrike Salzner,[3] Andrew J Musser,[4] Manish Jain,[5] Jyotishman Dasgupta,*[2] and Satish Patil*[1]

[1]Solid State and Structural Chemistry Unit, Indian Institute of Science, Bangalore 560012
[2]Department of Chemical Sciences, Tata Institute of Fundamental Research, Mumbai 400005, India
[3]Department of Chemistry, Bilkent University, Ankara 06800, Turkey
[4]Department of Physics and Astronomy, University of Sheffield, Sheffield, United Kingdom
[5]Department of Physics, Indian Institute of Science, Bangalore 560012
[†] denotes equal first authorship
*Correspondence to: dasgupta@tifr.res.in and spatil@iisc.ac.in
Present Address of Palas Roy: Department of chemistry, Northwestern University.

Abstract

The formation of two triplet excitons at the cost of one photon via singlet exciton fission in organic semiconductors can potentially enhance the photocurrent in photovoltaic devices. However, the role of spin density distribution in driving this photophysical process has been unclear until now. Here we present the significance of electronic spin density distribution in facilitating efficient intramolecular singlet exciton fission (iSEF) in π-bridged pentacene dimers. We synthetically modulate the spin density distribution in a series of pentacene dimers using phenyl-, thienyl- and selenyl- flanked diketopyrrolopyrrole (DPP) derivatives as π-bridges. Using femtosecond transient absorption spectroscopy, we find that efficient iSEF is only observed for the phenyl-derivative in ~2.4 ps while absent in the other two dimers. Electronic structure calculations reveal that phenyl-DPP bridge localizes α- and β-spin densities on distinct terminal pentacenes. Upon photoexcitation, a spin exchange mechanism enables iSEF from a singlet state which has an innate triplet pair character.

1

Introduction

Singlet exciton fission (SEF) is a spin allowed process that was first discovered in anthracene crystals in 1965.[1] It involves the absorption of one photon by a singlet ground state molecule, followed by separation of the photoexcited singlet excited state into two triplets residing on two different chromophores. SEF as a phenomenon was soon observed also in larger acene structures and discovered later in numerous other conjugated molecules.[2–5] The set of materials that demonstrate SEF is limited by the energy criterion that the singlet state energy (E_S) should be approximately two times or greater than the triplet energy (E_T) i.e. $E_S \geq 2E_T$, though the observation of endothermic fission in tetracene reveals some flexibility in this design principle.[5,6] In addition, the chromophores which satisfy the energy criterion have to be electronically coupled through optimal molecular packing.[7,8] Recently, the dependence of SEF efficiency on molecular packing was circumvented by the demonstration of intramolecular SEF (iSEF) in which the SEF chromophores are coupled via a covalent bridge.[9–11,12] The orientation of the covalently coupled chromophores plays a significant role in driving iSEF as exemplified by the observation that 1,3-diphenylisobenzofuran shows 200% SEF efficiency in crystals but the quantum yield reduces to 10% when they are covalently coupled.[13,14] Acene dimers have proven more fruitful, with several reports of nearly quantitative intramolecular singlet fission yields in a wide range of structures.[11,15–17] These species are evidence for tunability of rate and yield of iSEF, and even changes in underlying mechanism[16,17] through the electronic nature of the bonding interaction.

Extensive work has yielded a general consensus that SEF[11,17,18] proceeds via conversion of photoexcited spin singlet states (S_1) to dark multi-excitonic coupled triplet pair states (^1TT), in some cases mediated by charge-transfer states. The intermediate ^1TT pairs subsequently dissociate to generate pairs of free triplets (T) localized on different chromophores.[19–25] The correlated changes in the electronic states and their corresponding spin configurations in covalently coupled systems have, however been difficult to comprehend, thereby limiting the design principles. In order to systematically control electron delocalization with spin density distributions, we have synthesized new pentacene dimers with biradicaloid character[24,26,27] that possess energetically proximate singlet and triplet pair states. The two pentacenes were bridged by push-pull chromophores made of diketopyrrolopyrrole (DPP) linked with three different aryl π-groups: phenyl, thienyl and selenyl, (leading to 2P-PDPP, 2P-TDPP and 2P-SeDPP respectively). The

biradicaloid character of the molecular systems allows singlet to ^{1}TT pair mixing through the CT character of the backbone. Broadband femtosecond transient absorption measurements show that only the phenyl derivative undergoes iSEF, in the picosecond timescale. Theoretical analysis of the spin orbitals and S_1 states reveals that spin localization and consequently partial ^{1}TT character of S_1 explain the rapid singlet fission of the phenyl derivative.

Results

Steady-state electronic spectroscopy. The structures of 2P-PDPP, 2P-TDPP and 2P-SeDPP are given in Figure 1a. Synthetic procedures and characterization data are available as Supplementary Figure 1, 21-35 and Supplementary methods. UV-visible absorption spectra of the three compounds in chlorobenzene are presented in Figure 1b. All the three compounds absorb strongly over a broad range of the visible spectrum with contributions identifiable from the pentacene and bridging DPP units (Supplementary Figure 2). The sharp vibronic features of the components seen in 2P-PDPP are significantly broadened in 2P-TDPP and 2P-SeDPP, suggesting conformational heterogeneity. The absorption spectra of 2P-TDPP and 2P-SeDPP are also strongly red-shifted, a consequence of the longer conjugation enabled by the less-bulky 5-membered ring bridges, and exhibit more diffuse absorption. Electronic structure calculations using UTD-B3P86-30%/6-31G* in chlorobenzene reproduced the absorption peak positions with maximum error of 0.20 eV (Supplementary Figure 16). The calculations reveal that the spectral differences of 2P-TDPP and 2P-SeDPP compared to 2P-PDPP are caused by stronger delocalization of the frontier orbitals and smaller energy gaps.
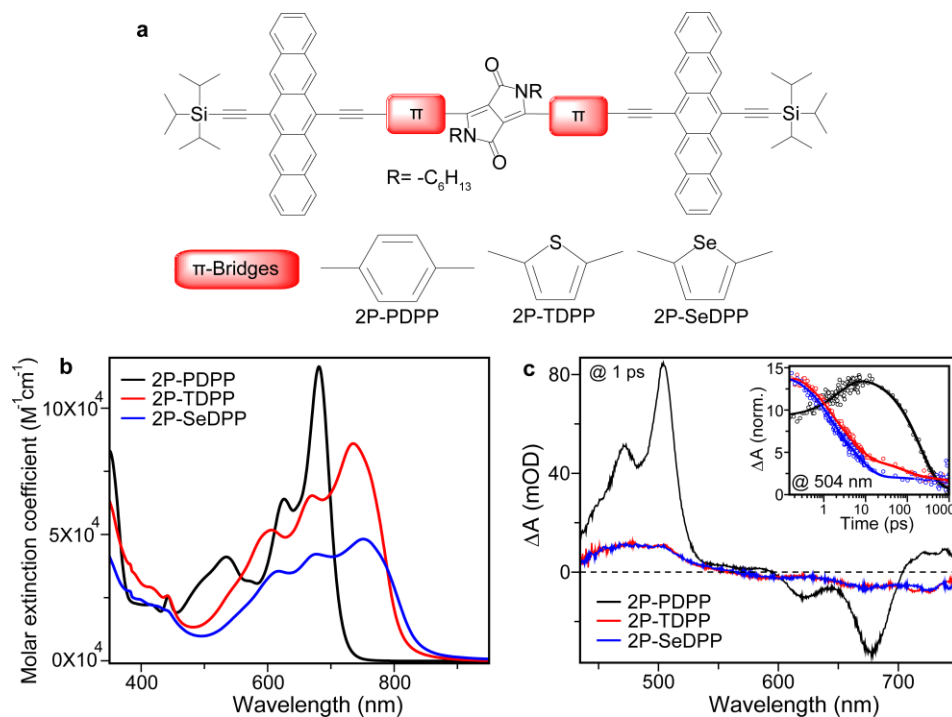
Figure 1: Design of pentacene dimers and their optical properties. (a) Chemical structures of 2P-PDPP, 2P-TDPP and 2P-SeDPP. (b) Steady-state absorption spectra of the three molecules; and (c) their transient absorption spectra (TA) collected at 1 ps pump-probe delay. All three molecules were dissolved in chlorobenzene at 25 μM concentration for the TA measurements, and excited using 0.1 mW pump pulses. For 2P-PDPP the excitation wavelength was 670 nm while it was 650 nm for both 2P-TDPP (red) and 2P-SeDPP (blue). Inset: Transient absorption kinetics taken at the photoinduced absorption peak at 504 nm.

Excited State Dynamics. Excited state spectra of 2P-PDPP, 2P-TDPP and 2P-SeDPP in chlorobenzene were investigated using broadband femtosecond transient absorption spectroscopy. In all the samples, we observe positive excited state absorption features (as shown in main Figure 1c and Supplementary Figure 6) between 450-550 nm, while the 550-750 nm spectral region is

4

dominated by ground state bleach peaks, which match the steady state absorption. We also observe a broad excited-state absorption in the NIR region from 850-1200 nm corresponding to the singlet manifold (Supplementary Figures S5-S6). In case of 2P-TDPP and 2P-SeDPP the instantaneously generated S_1 state exhibits surprisingly fast decay, a major fraction returning to the ground state with no obvious spectral evolution within the first few ps, as evident from the kinetics at 504 nm (Fig 1c inset) and in the NIR region (Supplementary Figure 7). However, 2P-PDPP exhibits a distinct 504 nm excited-state absorption peak along with a sharp shoulder centered at ~470 nm, thereby being completely distinguishable from the other two molecules (see Figure 1c). These features are correlated with a unique excited-state absorption peak at 955 nm (Supplementary Figure 5). Moreover, the kinetics of 2P-PDPP at 504 nm shows a rise representing the formation of a new state (inset, Figure 1c). In order to understand the excited state evolution of 2P-PDPP and to assign the character of the new photoproduct, we carried out detailed investigation of the recorded pump-probe dynamics. The temporal evolution of the excited state spectra is shown as a contour diagram in Figure 2a. Here, we can distinguish three prominent positive ΔA features with peaks at 478, 504 and 730 nm arising from different excited state absorption transitions. The transient spectral features at 478 and 504 nm rise for ~3 ps while the peak near 730 nm is instantaneously generated (Figure 2b and Supplementary Figure 5). The 955 nm peak and broad NIR excited-state absorption also form promptly with photoexcitation, with the broad absorption decaying in the sub-ps time scale as shown in Fig 2b. Following the initial fast process, the remaining excited-state absorption peaks in the visible and NIR regions decay together within ~ 1 ns.

Global analysis[28] of the 2P-PDPP TA data set in chlorobenzene reveals two components with lifetimes of 2.4 and 213 ps as shown in Figure 2c. The first species corresponds to the initially photoexcited S_1 state, and its decay can be directly resolved in the ESA in the near-infrared kinetics at 955 nm (Figure 2b). S_1 converts into the long-lived species characterized by sharp excited-state absorption at 504 nm with a time constant of 2.4 ps. This spectrum is reminiscent of triplet signatures in other pentacene materials and the sharp peak at 955 nm closely matches the triplet absorption of TIPS-pentacene in solution.[15,16,29,30] In order to confirm the assignment to triplets we performed flash photolysis. As shown in Figure 2c, the spectrum obtained at 50 ns (red dots) matches well with the ~213 ps component in the transient absorption data. The species in flash photolysis exhibits faster decay in the presence of atmospheric O_2 (Supplementary Figure 4),

confirming that the long-lived species following direct excitation of 2P-PDPP corresponds to triplet excitons. Interestingly, the characteristic triplet peak in the NIR is evident from the earliest time delays (Supplementary Figure 5), suggesting some triplet character in the initial photoexcitation; we return to this point below. In the absence of O_2 the triplet life time of 2P-PDPP solution in chlorobenzene is 8.6 μs. It is evident that some of the triplets formed by iSEF survive the fast (213 ps) recombination regime and persist on much longer timescales, similar to other bridged pentacene dimers.[11,15,31] Moreover, the sensitivity to O_2 reveals that the triplet energy is between 0.8 and 1 eV, similar to earlier reports of modified triplet energies in orthogonal pentacene dimers.[32]

To characterize the process, we have performed control experiments on pump power, solvent polarity etc. None of the observed behavior was found to change with excitation density, from 0.04 mW to 0.2 mW pump power (Supplementary Figure 8). Likewise, the kinetics are identical over the concentration range 10-100μM (Supplementary Figure 9) and DOSY-NMR (Supplementary Figure 12) reveals no appreciable aggregation of 2P-PDPP at the concentrations used for TA, confirming that the process observed is indeed intramolecular. Interestingly, the dynamics are affected by the choice of pump photon energy. When we selectively excite the PDPP bridging unit at 485 nm, we observe a markedly slower rise of the triplet ESA at 504 nm (8.6 ps rather than 2.4 ps, spectra and kinetics are shown in Supplementary Figure 10). This indicates that iSEF is only operative when the DPP-centric singlet state relaxes to the coupled pentacene S_1-state, thereby sensitizing the process beyond the conventional absorption window of the individual pentacenes. The process of excitation energy transfer through the bridge certainly is an exciting direction for designing new iSEF molecules which feature π-bridges as implicit chromophores exclusively.

Solvent Polarity Control of Singlet Fission. In order to probe the mechanistic pathway of iSEF and particularly the role of CT states in mediating the coupling,[16] we have performed solvent-dependent TA of 2P-PDPP. We have used a range of solvents including chloroform, chlorobenzene, toluene and cyclohexane as well as two solvent mixtures. Figure 2d shows a comparison of transient absorption spectra of 2P-PDPP at 1 ps pump-probe delay in a range of mixtures of chlorobenzene and cyclohexane. In pure cyclohexane, only the S_1 signature can be observed on these timescales; indeed, no iSEF is observed in cyclohexane even at much longer

delays (Supplementary Figure 13). It is evident that the sharp triplet state absorption near 504 nm emerges gradually as the polarity of the medium increases.
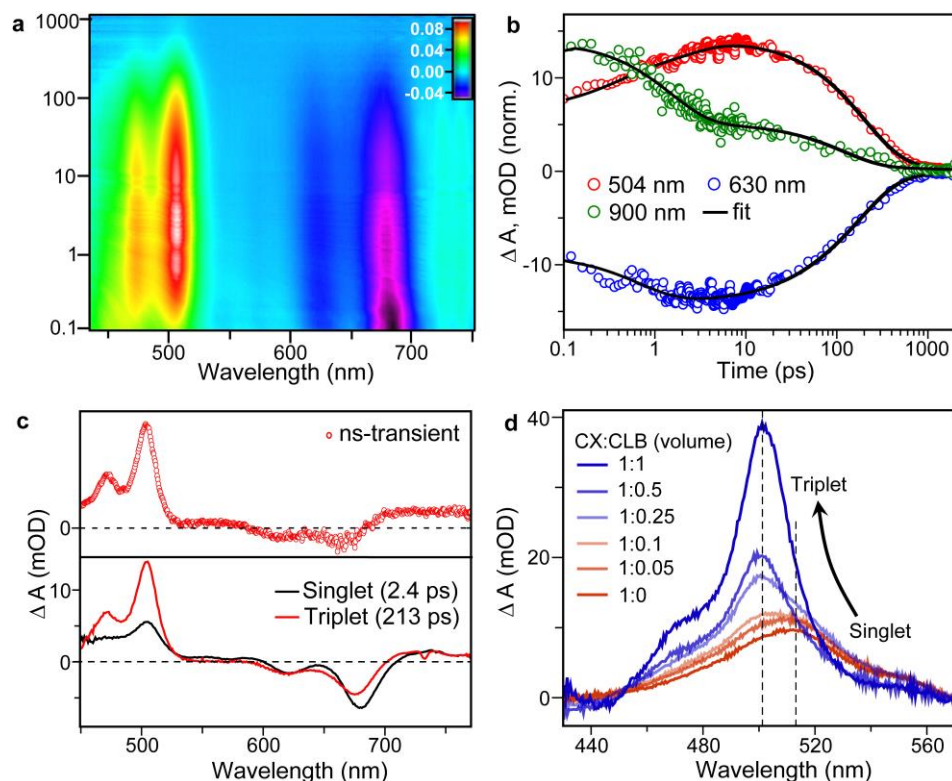

Figure 2: Excited state dynamics of 2P-PDPP and solvent polarity control of SEF. (a) Contour diagram of the obtained broadband transient absorption spectra in between 50 fs to 1 nanosecond subsequent to 670 nm excitation. (b) Single wavelength kinetics at 504, 630 and 900 nm. Symbols are raw data and lines are multi-exponential fits from single wavelength kinetics analysis. (c) Singlet and triplet species associated spectra obtained from global analysis are compared to the nanosecond transient absorption spectrum experimentally obtained using flash photolysis. (d) The shift and growth of excited-state absorption at 1ps pump-probe delay with solvent polarity in mixtures of cyclohexane (CX) and chlorobenzene (CLB).

Multiexcitonic Bright State of 2P-PDPP. To establish whether the molecules satisfy the energy criterion for singlet fission ($E_{S1} \geq 2E_T$), we calculated the adiabatic excited states of 2P-PDPP, 2P-TDPP and 2P-SeDPP with time-dependent density functional theory (TDDFT) (theoretical methods are described in Methods section). The excitation energies are 1.68 eV, 1.49 eV, and 1.44 eV, respectively. As iSEF creates triplets that are located on the pentacenes, we calculated the vertical triplet energies of the TIPS-pentacene fragments including the acetylene unit (end-capped with an H atom). For triplet energy calculations, we used the ΔSCF method. The first triplet state of the TIPS-pentacene fragments lies 0.69 eV above S_0. With a singlet energy requirement of 1.38 eV for creating two triplets, singlet fission from S_1 should be feasible in all three molecules and should be fastest for 2P-TDPP and 2P-SeDPP because $2 \times E_T$ and E_{S1} are almost identical. Though these calculated values slightly underestimate the measured S_1 energies and E_T of TIPS-pentacene[25], the trends are correctly reproduced. Moreover, we note that iSEF would also be energetically accessible for all three molecules on the basis of the measured S_1 energies and E_T of TIPS-pentacene (~0.8 eV) obtained from phosphorescence measurement,[25] particularly given the energetic stabilization of the ^{1}TT state relative to $2E_T$.[21,24,25,33]

Analysis of the ground-state wave functions reveals that all three molecules have biradicaloid ground states, i.e. they have significant resonance contributions from biradical structures. Therefore, we focus specifically on the spin properties of the excited states of 2P-PDPP, 2P-TDPP, and 2P-SeDPP and describe them in terms of the spin orbitals (SOs) for α- and β-electrons. As such, α and β-electrons have the same energy but reside in SOs that are symmetry equivalents and tend to be localized on opposite ends of the molecules. In Figure 3a the frontier SOs of 2P-PDPP are plotted in order of increasing energy. The highest occupied spin orbitals (HOSO) and HOSO-1 and the lowest unoccupied spin orbitals (LUSO) and LUSO+1 are localized mostly on pentacene. HOSO-1 and HOSO as well as LUSO and LUSO+1 are very close in energy. The S_1 state does not arise from a single HOSO-LUSO transition but rather, like all excitations with energies up to 520 nm, from a linear combination of transitions involving HOSO, HOSO-1, LUSO, and LUSO+1. As in closed-shell calculations, α- and β-electrons contribute equally.

For 2P-PDPP the largest contribution to S_1 (64%) comes from the HOSO-LUSO transitions. From Figure 3, it is clear that due to the localized nature of α and β SOs on opposite pentacenes, the HOSO-LUSO transitions of α- and β-electrons individually have charge-transfer (CT) character

and their superposition creates a CR state. The net effect of the CR process is to exchange the electron spins between the pentacenes without creating any charge separation. If the HOSO-LUSO CR transitions were the only contributions to S_1, 2P-PDPP would be in the ^{1}TT state directly after photoexcitation. However, there are additional contributions to S_1: HOSO-1 to LUSO+1 (13%), (a CR state in reverse direction compared to HOSO-LUSO), plus local excitations (LE) HOSO to LUSO+1 (12%), and HOSO-1 to LUSO (8%). The LE contributions to S_1 are essential because the large spatial overlap between HOSO and LUSO+1 and between HOSO-1 and LUSO contributes oscillator strength to S_1.

Taking all the contributions together and factoring HOSO to LUSO and HOSO-1 to LUSO+1 CR states move the electrons in opposite directions, the strongly allowed S_1 state has 77% CR and at least 50% ^{1}TT character. The electron density on the bridge increases by 0.14 eV during excitation to S_1. Indeed, the PDPP bridge is crucial in bringing about the coupling between LE and CR states, a finding which is independent of the density functional used (global hybrid or range-separated, Supplementary Figure 17). We therefore conclude that S_1 is a superposition of LE and CR states resulting in a partial ^{1}TT character of the bright S_1 state.

Discussion

Based on the ultrafast triplet formation kinetics in 2P-PDPP, we invoke iSEF as the generation pathway. This can also be inferred from the subsequent triplet decay within hundreds of picoseconds (213 ps), which can only be rationalized through intramolecular triplet-triplet annihilation. In a dimer such as 2P-PDPP the triplets generated by iSEF will reside on the two pentacene units, separated by the PDPP bridge. In pentacene dimers reported earlier, it has been demonstrated that the absorption signatures of the coupled triplet-pair states ^{1}TT cannot be distinguished from free or uncoupled triplets if the inter-chromophore separation is more than few C-C single bonds.[31] In 2P-PDPP the triplet pair is spatially separated by the length scale of the π-PDPP-π bridge, a distance of ~1 nm. At this spacing free triplets and a weakly coupled ^{1}TT pair would be spectrally identical. However, the rapid geminate annihilation behavior is most consistent with the coupled pair state,[34] and we thus assign the signature obtained at 1 ps specifically to weakly coupled triplet pairs.

The solvent polarity dependence of singlet fission can be rationalized by invoking a charge resonance (CR) character of the S_1-state in 2P-PDPP that arises from a superposition of charge transfer processes between the two terminal pentacenes (as described in the theoretical section). In the other two derivatives, the S_1 states do not have CR character (see below) and we observe neither iSEF nor any solvent dependence. This idea was independently tested by mixing two solvents that support iSEF but show different rates. We found that the triplet generation in toluene is slowed down considerably as compared to chlorobenzene. This rate increases when chlorobenzene is titrated with toluene (Supplementary Figure 14) clearly indicating the role of CR states in dictating the iSEF process. This indicates that the PDPP bridge plays a critical role in facilitating the CT coupling in the multi-excitonic singlet state.

It is important to recognize that although 2P-TDPP and 2P-SeDPP have biradicaloid ground states, neither of them undergoes iSEF. We conjecture that the inhibition of iSEF arises from the electronic nature of the SOs. The α-HOSOs of 2P-PDPP and 2P-TDPP are shown in Figure 3b. Supplementary Figure 18 compares additional frontier α-SOs of 2P-PDPP with those of 2P-TDPP and 2P-SeDPP (β-SOs are not shown as they are symmetry equivalents of the α-SOs). It is clearly visible that HOSOs and especially LUSOs of 2P-TDPP and 2P-SeDPP are delocalized, having less spin density on pentacene, and stronger contributions from the bridges. Because of this delocalization, HOSO to LUSO transitions, which dominate S_1 of 2P-TDPP and Se-PDPP with contributions of 87% and 85% respectively, have little CR character and do not exchange spins across the molecules. Hence, unlike in 2P-PDPP, the S_1 states of 2P-TDPP and 2P-SeDPP do not have [1]TT character. To which extent the spin distributions depend on the planar structures of 2P-TDPP and 2P-SeDPP as compared to the non-planar structure of 2P-PDPP was tested by calculating 2P-PDPP in planar and 2P-SeDPP in non-planar form. For 2P-PDPP the CR character of S_1 increases on planarization, while breaking the planarity of 2P-SeDPP results in further localization of the LUSO on the pentacenes. Interestingly, distortion from the equilibrium geometry thus appears to favor iSEF in both molecules. Hence, our observed differences are not simply a function of planarity. These computational results are shown in SI (Supplementary Figure 19).
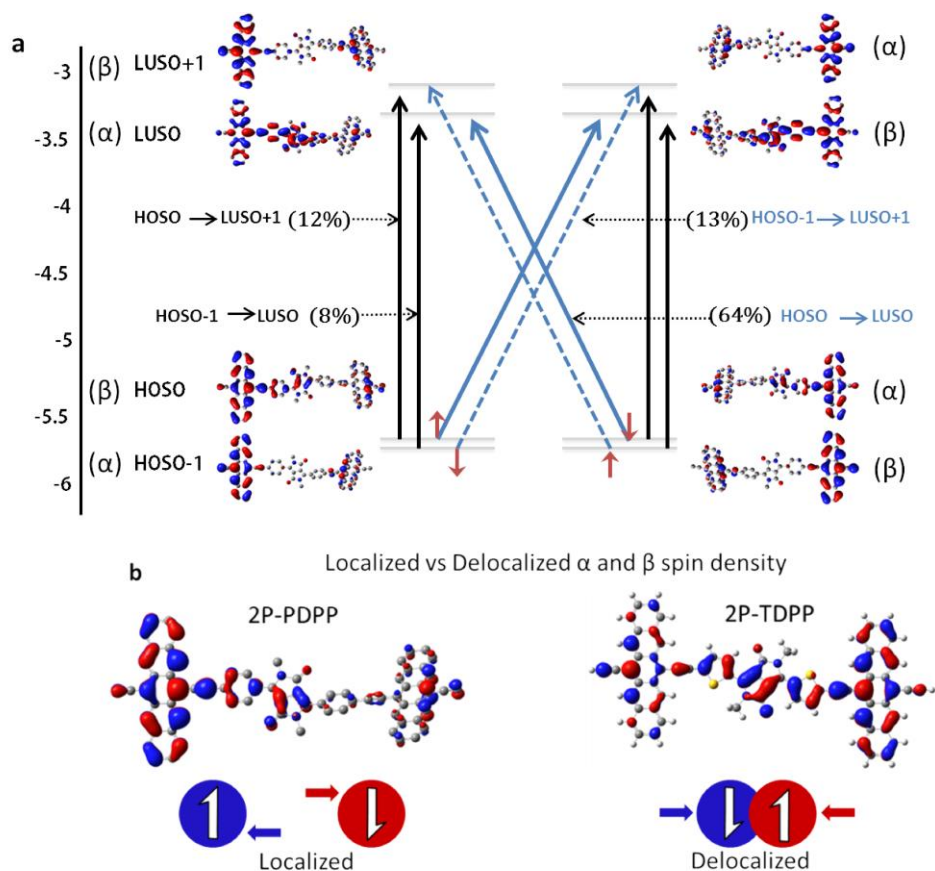
Figure 3: **Contributions of orbital replacements and spin density comparison.** (a) The electron density change between ground and excited state arises from a linear combination of orbital replacements with CT (blue arrows) and LE (black arrows) character. The HOSO to LUSO transition which contributes strongest (64%), has CR character, moving the α-electron from left to right and the β- electron from right to left. This leads to a partial ^{1}TT character of S_1. (b) α-HOSOs of 2P-PDPP and 2P-TDPP (the symmetry equivalent β− orbitals are omitted). In 2P-PDPP α- and β- electrons are spatially separated because the SOs are polarized towards opposite pentacenes. In 2P-TDPP the SOs of α−and β−electrons are less polarized and involve the bridge more strongly.

Vibronic mixing of S_1 and ^1TT has been suggested to explain 2D photon echo measurements of pentacene films[35] and rapid endothermic SEF in TIPS-tetracene.[21] Here, we did not consider any vibrational coupling but find that biradical character is essential as CR states can not occur in closed-shell molecules, where α- and β- electrons occupy identical space orbitals. Compared to CT-mediated coupling of S_1 and ^1TT states discussed in the literature,[9,10,16,36] there are three main differences in the present work: the CR character occurs directly in S_1 rather than evolving from S_1; Due to the simultaneous CTs in opposite directions, no ion pairs are formed and the energy of the CR state is lower than that of a CT state; Unlike the CT mediated mechanism, which requires further electron transfer to reach ^1TT, the present mechanism requires no further intermediate states as S_1 already has partial ^1TT character and can therefore relax very fast to the lower lying ^1TT state. We propose that this process can be described adiabatically[8,33], where relaxation along the S_1-^1TT potential energy surface from the Franck-Condon point results in gradual increase of the ^1TT character of the wave function. We thus observe triplet excited state absorption signatures in the NIR instantaneously upon photoexcitation, while the triplet signatures at shorter wavelengths grow as the system relaxes into the ^1TT minimum.[37,38] It should be noted that the triplet pair state formed at picosecond timescale is a relaxed and weakly coupled state, which has an almost "free" triplet-like transient signature. The reason for this unusual behavior is the nature of the PDPP bridge that sufficiently couples the pentacenes but contributes little enough to the frontier SOs to facilitate a partial exchange of α- and β-electrons during photoexcitation. Subtle changes in solvent polarity or of the donor units in the bridge increase delocalization and prevent iSEF.

To establish whether this mechanism is unique to 2P-PDPP, we have investigated other pentacene dimers as reported by Lukman, S. *et al.*[16], Sanders, S. N., *et. al.*[31], and Zirzlmeier, J. et al.[29] In addition, we modified 2P-PDPP by replacing pentacene with tetracene, hexacene, and heptacene (Supplementary Figure 20). According to our preliminary results, all of the systems with exception of the tetracene analog of 2P-PDPP (molecule 11 in Supplementary Figure 20) have biradical ground states. The nature of the SOs depends strongly on the mode of coupling, the orientation of the pentacenes, and the length of the spacer. When pentacenes are directly coupled and perpendicular to one another (molecules 1 and 2 in Supplementary Figure 20), S_1 and CT states do not mix. S_1 is localized on pentacenes and has low oscillator strength (0.20). Pure CT states with zero oscillator strength are found at about 0.3 eV above S_1 with the range separated hybrid

functional wB97-XD[16]. In end-to-end linked biphenyl (molecule 3 in Supplementary Figure 20) spin densities are only partially localized. S_1 has CR character but low oscillator strength (0.23). This system was found experimentally to undergo rapid singlet fission but also rapid triplet-triplet annihilation[31]. With phenyl spacers of increasing length (molecule 4, 5 and 10 in S20), localization increases and CR character of S_1 decreases. Only when the pentacenes are coupled to phenyl through acetylene groups[29] (molecules 6-9, 11 and 12 in S20), the oscillator strength of S_1 gets larger with the following substitution pattern: meta (0.38) < ortho (0.57) < para (0.85) while S_1 has a strong CR character. With hexacene and heptacene instead of pentacene, spin densities are localized but CR character and oscillator strength of S_1 are less than with pentacene. This is in line with longer acenes being less efficient SEF chromophores[39]. Thus although most of these systems undergo iSEF, spin density appears to be crucial in controlling iSEF rates, triplet-triplet annihilation, and oscillator strength of S_1. Among these systems, 2P-PDPP is unique because of its unusually large oscillator strength of S_1 (1.28). Detailed investigations of the above systems and correlation with experimental data are currently under way in our labs and will be subject to forthcoming publications. If spin density distribution of the frontier molecular orbitals will turn out to offer important insight into ultrafast iSEF processes in general, it may become a critical aspect to rationally design new materials.

Commented [WU1]: Maybe we can use this modification as toning down our claims? What do you think?

In summary, we have demonstrated here the synthetic control of spin density localization in three pentacene dimers by tuning the electronic nature of the π-bridge, and thereby enabling iSEF. With the optimized PDPP bridge, the partitioning of spin density on opposite sides of the dimer afforded a new coherent spin exchange mechanism, endowing the strongly absorbing S_1 state with partial [1]TT character. We have focused here specifically on covalent dimers, due to the ease of synthetic tuning and their computational tractability. However, there is no intrinsic barrier to the extension of this design principle and fission mechanism to the more common solid-state systems. We anticipate that spin density localization will prove relevant in those as well, recalling for instance the comparable contribution of equal and opposite charge transfer configurations to the lowest singlet state in crystalline pentacene.[36,40] Indeed, the important role of mixing S_1, CT and [1]TT states similar to that revealed by our calculations was recently invoked for heteroacene[21,25] and zethrene[24] thin films, pentacene dimers[16] and terrylene bisimide dimers[41]. It is beyond the scope of our current investigation to determine whether this mixing is accompanied by similar spin density localization effects, but this is an important question for further study that may reveal a

more general mechanistic principle. This emergent mechanism should motivate new time-resolved experiments for spin-state tracking in SEF-active materials, while bringing into focus the use of chromophoric bridges, which can simultaneously act as antennas for sensitizing iSEF and fine-tune the properties that enable fission. It has not escaped our attention that the reported coherent spin-exchange mechanism may also be critical in the development of organic materials for light-activated superconductivity where biexciton generation and its transport need to be optimized.

Methods

Materials. All the precursor materials used for synthesis of the three pentacene derivatives were obtained from commercial source and used without further purification; Solvents used for were dried and distilled out before being used for the synthesis of the molecules. 2P-PDPP, 2P-TDPP, and 2P-SeDPP were synthesized by two step processes starting from precursors through Sonogashira coupling followed by aromatization. Experimental procedure and synthetic methods are described in Supplementary Note 1. Intermediates and final compounds were purified by silica gel chromatography; structures and their purity were verified by 1H, 13C NMR, and MALDI-TOF.

Steady-state absorption and emission spectroscopy. UV–Vis spectra were recorded on Perkin-Elmer (Lambda 35) UV–Vis Spectrometer. Steady state fluorescence emission studies were carried out with a Spex FluoroLog-3 spectrofluorometer (Jobin- Yvon Inc.).

Flash-photolysis experiment. Laser Kinetic Spectrometer (Edinburgh Instruments, UK, model LP920) was used for nanosecond flash photolysis experiments at BARC, Mumbai. The sample in a 1 cm × 1 cm cuvette was pumped using a 7 ns laser pulse at 532 nm generated using a frequency doubled Nd-YAG laser (Thales Laser SA, France, model: SAGA). A pulsed 450 W xenon arc lamp generates the white light continuum (300−1000 nm) probe pulses.

Transient absorption measurements. The detailed description about the home-built pump-probe/ transient absorption setup has been described in detail earlier.[48] Briefly, a modelocked Ti:Sapphire laser oscillator (Coherent Micra-5 system) produces the fundamental laser pulse with 100 nm bandwidth, 27 fs pulse width, 80 MHz repetition rate, and 5 nJ/pulse power which was then amplified using a regenerative amplifier (Coherent Legend Elite®) to generate amplified

pulses with 60 nm bandwidth, 1 kHz repetition rate, 30 fs pulse width and 4 mJ/pulse power. Part of this amplified femtosecond pulse was guided through an ultrafast optical parametric amplifier system (Coherent OPeraASolo®) to generate tunable pump pulses which were used to excite the molecules of interest. Another part of the fundamental beam was passed through a 2 mm thick sapphire crystal to generate white-light probe continuum. The visible part (420-750 nm) of the broadband probe continuum was separated using a 800 nm short-pass filter while the NIR regimes (850-1300 nm) was selected using a 850 nm long pass filter. The actinic pump and probe pulses were focused and overlapped on the sample inside a flow cuvette with 2 mm glass window. The transmitted probe after the sample was dispersed using Helios® spectrograph onto an imaging element. The temporal resolution for the set up was determined to be near 90 fs. All pump-probe measurements were performed under flowing condition with the liquid driven by a peristaltic pump which ensures fresh sample before every laser shot. Pump pulse energy was attenuated to 100 nJ in order to minimize the photo-damage.

Theoretical methods. Ground and excited states of 2P-PDPP, 2P-TDPP, and 2P-SeDPP were investigated with density functional theory (DFT) and time-dependent DFT (TDDFT). Test calculations with and without the triisopropylsilyl (TIPS) groups show that TIPS groups influence neither singlet-triplet splitting nor excitation energies. Likewise replacing alkane chains with methyl groups does not influence the electronic structure (SI Figure S10). Therefore, the truncated systems were used for most of the calculations. As low lying excited states of large π-systems are not diffuse, the 6-31G* basis set was used throughout. Based on previous experience with conjugated and biradicaloid conjugated systems and further test calculations, the B3P86 functional with 30% of exact exchange was chosen.[41,42] Solvent effects of chlorobenzene and cyclohexane were included with the polarized continuum model (PCM) as implemented in Gaussian 09. All calculations are done with Gaussian 09, Rev. A 02.[43]

To characterize the ground states, closed-shell wave functions were checked for stability. Closed-shell wavefunctions of all three molecules have internal instabilities. At the B3P86-30%/6-31G* level the biradicaloids lie 0.02 eV (2.4 kJ/mol), 0.05 eV (4.8 kJ/mol), and 0.12 eV (11.9 kJ/mol) below the closed-shell forms for 2P-PDPP, 2P-TDPP, and 2P-SeDPP, respectively. This raises the issue of applicability of broken symmetry DFT (BS-DFT) as biradicals have two-detrimental wave functions while DFT uses only a single Slater determinant. Davidson and Clark

investigated biradicals and concluded that for large systems for which multi-reference methods cannot be employed, BS-DFT is the best choice of method.[44] Casida showed that excited state calculations with BS-TDDFT are reliable as long as the spin is conserved.[45] The applicability of TDDFT for states relevant to singlet fission of medium-sized biradicaloid systems was scrutinized vs. multi-reference approaches by Grotjahn et al.[46] The study confirms that single reference methods are reliable and that global hybrids are only marginally worse than local hybrids for singlet states. For triplets, the ΔSCF method was shown to yield reliable triplet energies.

Following the above studies, we calculated the triplet energies with the ΔSCF method as energy differences between BS-singlet and triplet ground states. We also confirm the applicability of BS-TDDFT as we observe no spurious or missing states in the BS-TDDFT absorption spectrum 2P-PDPP compared to the closed-shell spectrum (SI Figure S10), although the BS ground state has an expectation value of the spin operator of 0.95.

Analysis of the S_1 state of 2P-PDPP reveals a significant amount of charge transfer (CT) character. This touches another issue of TDDFT, the known underestimation of the energy of charge transfer states.[47] To assure that the CT admixture to S_1 is not an artefact, we compared absorption spectra of 2P-PDDP and of two different fragments obtained from 2P-PDPP by removing first the DPP bridge (fragment 2) and second also the phenyl groups (fragment 1) without reoptimizing the rest of the structure. This produces separate the locally excited (LE) and the CT states for the fragments. SI Figure S11 shows structures, excitation energies, and calculated spectra. Excited state calculations in the gas phase for the fragments with the B3P86-30% and the wB97X-D functionals predict LE states at 1.91 eV and 1.83eV with B3P86-30% and at 2.21 eV and 2.22eV with wB97X-D. These LE states have exactly the same energies as the corresponding excitations of the individual molecules. The fragments, however, have additional CT states at 2.49 eV (fragment 1) and 2.30 eV (fragment 2) with B3P86-30% and at 4.64 eV and 4.38 eV, respectively with wB97X-D. The wB97X-D CT states match the energy difference between ionization potential (IP) and electron affinity (EA) of 4.72 eV closely but the B3P86-30% CT excitation energies are lower than IP-EA of 3.75eV, as expected. Although wB97X-D predicts CT states correctly at much higher in energy, the S_1 state of 2P-PDPP is composed of a linear combination of LE and CT excitations with both functionals. S_1 is predicted at 1.68 eV (B3P86-30%) and at 2.10 eV (wB97X-D). Such increases in energy are observed generally with range-

separated funstionals.[1] With both functionals no pure CT states similar to those of the fragments are obtained. The admixture of CT excitations to S_1 is therefore not an artefact of the B3P86-30% functional. This indicates that incorporation of the DPP bridge changes the character of the S_1 state, leading to a red shift and a large increase in oscillator strengths. Comparing the B3P86-30% and wB97X-D spectra with the experimental one, reveals that the B3P86-30% absorption spectrum is in much better agreement with experiment in terms of peak positions, peak spacings, and relative oscillator strengths. Therefore, the B3P86-30% functional is used hereafter.

Data availability. The data sets generated and analyzed during the current study are available from the corresponding authors on reasonable request.

References

1. Singh, S., Jones, W. J., Siebrand, W., Stoicheff, B. P. & Schneider, W. G. Laser Generation of Excitons and Fluorescence in Anthracene Crystals. *J. Chem. Phys.* **42,** 330–342 (1965).

2. Rademaker, H., Hoff, A. J., Van Grondelle, R. & Duysens, L. N. M. Carotenoid triplet yields in normal and deuterated Rhodospirillum rubrum. *Biochim. Biophys. Acta - Bioenerg.* **592,** 240–257 (1980).

3. Swenberg, C. E. & Stacy, W. T. Bimolecular radiationless transitions in crystalline tetracene. *Chem. Phys. Lett.* **2,** 327–328 (1968).

4. Wilson, M. W. B. *et al.* Ultrafast Dynamics of Exciton Fission in Polycrystalline Pentacene. *J. Am. Chem. Soc.* **133,** 11830–11833 (2011).

5. Smith, M. B. & Michl, J. Singlet Fission. *Chem. Rev.* **110,** 6891–6936 (2010).

6. Smith, M. B. & Michl, J. Recent Advances in Singlet Fission. *Annu. Rev. Phys. Chem.* **64,** 361–386 (2013).

7. Le, A. K. *et al.* Singlet Fission Involves an Interplay between Energetic Driving Force and Electronic Coupling in Perylenediimide Films. *J. Am. Chem. Soc.* **140,** 814–826 (2018).

8. Yost, S. R. *et al.* A transferable model for singlet-fission kinetics. *Nat. Chem.* **6,** 492–497 (2014).

9. Margulies, E. A. *et al.* Enabling singlet fission by controlling intramolecular charge transfer in π-stacked covalent terrylenediimide dimers. *Nat. Chem.* **8,** 1120–1125 (2016).

10. Busby, E. *et al.* A design strategy for intramolecular singlet fission mediated by charge-transfer states in donor–acceptor organic materials. *Nat. Mater.* **14,** 426–433 (2015).

11. Basel, B. S. *et al.* Unified model for singlet fission within a non-conjugated covalent pentacene dimer. *Nat. Commun.* **8,** 15171 (2017).

12. Musser, A. J. A. J. *et al.* Activated singlet exciton fission in a semiconducting polymer. *J. Am.*

Chem. Soc. **135,** 12747–12754 (2013).

13. Johnson, J. C. *et al.* Toward Designed Singlet Fission: Solution Photophysics of Two Indirectly Coupled Covalent Dimers of 1,3-Diphenylisobenzofuran. *J. Phys. Chem. B* **117,** 4680–4695 (2013).

14. Schrauben, J. N., Ryerson, J. L., Michl, J. & Johnson, J. C. Mechanism of Singlet Fission in Thin Films of 1,3-Diphenylisobenzofuran. *J. Am. Chem. Soc.* **136,** 7363–7373 (2014).

15. Kumarasamy, E. *et al.* Tuning Singlet Fission in π-Bridge-π Chromophores. *J. Am. Chem. Soc.* **139,** 12488–12494 (2017).

16. Lukman, S. *et al.* Tuning the role of charge-transfer states in intramolecular singlet exciton fission through side-group engineering. *Nat. Commun.* **7,** 13622 (2016).

17. Fuemmeler, E. G. *et al.* A Direct Mechanism of Ultrafast Intramolecular Singlet Fission in Pentacene Dimers. *ACS Cent. Sci.* **2,** 316–324 (2016).

18. Tayebjee, M. J. Y. J. Y. *et al.* Quintet multiexciton dynamics in singlet fission. *Nat. Phys.* **13,** 182–188 (2017).

19. Chan, W. L. *et al.* Observing the multiexciton state in singlet fission and ensuing ultrafast multielectron transfer. *Science (80-.).* **334,** 1541–1545 (2011).

20. Zimmerman, P. M., Bell, F., Casanova, D. & Head-Gordon, M. Mechanism for Singlet Fission in Pentacene and Tetracene: From Single Exciton to Two Triplets. *J. Am. Chem. Soc.* **133,** 19944–19952 (2011).

21. Stern, H. L. *et al.* Vibronically coherent ultrafast triplet-pair formation and subsequent thermally activated dissociation control efficient endothermic singlet fission. *Nat. Chem.* **9,** 1205–1212 (2017).

22. Scholes, G. D. Correlated Pair States Formed by Singlet Fission and Exciton–Exciton Annihilation. *J. Phys. Chem. A* **119,** 12699–12705 (2015).

23. Pensack, R. D. *et al.* Observation of Two Triplet-Pair Intermediates in Singlet Exciton Fission. *J. Phys. Chem. Lett.* **7,** 2370–2375 (2016).

24. Lukman, S. *et al.* Efficient Singlet Fission and Triplet-Pair Emission in a Family of Zethrene Diradicaloids. *J. Am. Chem. Soc.* **139,** 18376–18385 (2017).

25. Yong, C. K. K. *et al.* The entangled triplet pair state in acene and heteroacene materials. *Nat. Commun.* **8,** 15953 (2017).

26. Minami, T., Ito, S. & Nakano, M. Fundamental of Diradical-Character-Based Molecular Design for Singlet Fission. *J. Phys. Chem. Lett.* **4,** 2133–2137 (2013).

27. Minami, T. & Nakano, M. Diradical Character View of Singlet Fission. *J. Phys. Chem. Lett.* **3,** 145–150 (2012).

28. Snellenburg, J. J., Laptenok, S. P., Seger, R., Mullen, K. M. & Stokkum, I. H. M. van. Glotaran : A Java -Based Graphical User Interface for the R Package TIMP. *J. Stat. Softw.* **49,** 1–22 (2012).

29. Chiyotani, K. The natural history of pneumoconiosis. *Respir. Circ.* **36,** 955–959 (1988).

30. Walker, B. J., Musser, A. J., Beljonne, D. & Friend, R. H. Singlet exciton fission in solution. *Nat. Chem.* **5,** 1019–1024 (2013).

31. Sanders, S. N. *et al.* Quantitative Intramolecular Singlet Fission in Bipentacenes. *J. Am. Chem. Soc.* **137,** 8965–8972 (2015).

32. Lukman, S. *et al.* Tuneable Singlet Exciton Fission and Triplet-Triplet Annihilation in an Orthogonal Pentacene Dimer. *Adv. Funct. Mater.* **25,** 5452–5461 (2015).

33. Feng, X., Luzanov, A. V. & Krylov, A. I. Fission of entangled Spins: An electronic structure perspective. *J. Phys. Chem. Lett.* **4,** 3845–3852 (2013).

34. Sanders, S. N. *et al.* Exciton Correlations in Intramolecular Singlet Fission. *J. Am. Chem. Soc.* **138,** 7289–7297 (2016).

35. Bakulin, A. A. *et al.* Real-time observation of multiexcitonic states in ultrafast singlet fission using coherent 2D electronic spectroscopy. *Nat. Chem.* **8,** 16–23 (2016).

36. Beljonne, D., Yamagata, H., Brédas, J. L., Spano, F. C. & Olivier, Y. Charge-transfer excitations steer the davydov splitting and mediate singlet exciton fission in pentacene. *Phys. Rev. Lett.* **110,** 226402 (2013).

37. Grieco, C. *et al.* Direct Observation of Correlated Triplet Pair Dynamics during Singlet Fission Using Ultrafast Mid-IR Spectroscopy. *J. Phys. Chem. C* **122,** 2012–2022 (2018).

38. Grieco, C. *et al.* Harnessing Molecular Vibrations to Probe Triplet Dynamics during Singlet Fission. *J. Phys. Chem. Lett.* **8,** 5700–5706 (2017).

39. Busby, E. *et al.* Multiphonon relaxation slows singlet fission in crystalline hexacene. *J. Am. Chem. Soc.* **136,** 10654–10660 (2014).

40. Yamagata, H. *et al.* The nature of singlet excitons in oligoacene molecular crystals. *J. Chem. Phys.* **134,** 204703 (2011).

41. Ray, S., Sharma, S., Salzner, U. & Patil, S. Synthesis and Characterization of Quinoidal Diketopyrrolopyrrole Derivatives with Exceptionally High Electron Affinities. *J. Phys. Chem. C* **121,** 16088–16097 (2017).

42. Salzner, U. & Aydin, A. Improved prediction of properties of π-conjugated oligomers with range-separated hybrid density functionals. *J. Chem. Theory Comput.* **7,** 2568–2583 (2011).

43. MJF. G09 | Gaussian.com. Available at: http://gaussian.com/glossary/g09/. (Accessed: 3rd October 2018)

44. Davidson, E. R. & Clark, A. E. Spin polarization and annihilation for radicals and diradicals. *Int. J. Quantum Chem.* **103,** 1–9 (2005).

45. Ipatov, A., Cordova, F., Doriol, L. J. & Casida, M. E. Excited-state spin-contamination in time-dependent density-functional theory for molecules with open-shell ground states. *J. Mol. Struct. THEOCHEM* **914,** 60–73 (2009).

46. Grotjahn, R., Maier, T. M., Michl, J. & Kaupp, M. Development of a TDDFT-Based Protocol with Local Hybrid Functionals for the Screening of Potential Singlet Fission Chromophores. *J. Chem. Theory Comput.* **13,** 4984–4996 (2017).

47. Dreuw, A., Weisman, J. L. & Head-Gordon, M. Long-range charge-transfer excited states in time-dependent density functional theory require non-local exchange. *J. Chem. Phys.* **119,** 2943–2946 (2003).

48. Roy, P., Jha, A. & Dasgupta, J. Photoinduced charge generation rates in soluble P3HT : PCBM nano-aggregates predict the solvent-dependent film morphology. *Nanoscale* **8,** 2768–2777 (2016).

Author contributions

S. P. conceived the research while K.C.K. and P.R. performed the experiments and analyzed the experimental data with contributions from J.D. The pentacene derivatives were synthesized by K.C.K. and B.P. The computational work was done by U.S…… The manuscript was written by J.D., P.R., S.P., K.C.K., U.S. in consultation with A.J.M. and M.J. All the co-authors read and agreed with the final version of the manuscript.

Additional information

Supplementary information accompanies this paper at http://www.nature.com/naturecommunications

Competing financial interest: The authors declare no competing financial interests.

Materials and Correspondence should be addressed to J.D. and S.P.